JBC Papers in Press. Published on May 18, 2017 as Manuscript M116.764670
The latest version is at http://www.jbc.org/cgi/doi/10.1074/jbc.M116.764670

Coagulation factor VIIa–mediated protease-activated receptor 2 activation leads to β-catenin accumulation via the AKT/GSK3β pathway and contributes to breast cancer progression

Abhishek Roy[¥], Shabbir A. Ansari[¥], Kaushik Das[¥], Ramesh Prasad[¥], Anindita Bhattacharya[¥], Suman Mallik[¥], Ashis Mukherjee[†] and Prosenjit Sen[¥,*]

From the [¥]Department of Biological Chemistry, Indian Association for the Cultivation of Science, Kolkata-700032, India.[†]Netaji Subhash Chandra Bose Cancer Research Institute, Kolkata-700016, India

Running title: TF-FVIIa induced breast cancer metastasis

[*]To whom correspondence should be addressed: Dr. Prosenjit Sen, Department of Biological Chemistry, Indian Association for the Cultivation of Science, 2A & 2B Raja S. C. Mullick Road, Jadavpur, Kolkata-700032, India, Telephone:+913324734971; FAX:+913324732805; E-mail: bcps@iacs.res.in

Keywords: β-Catenin, Breast Cancer, Coagulation Factor, Metastasis, Protease-Activated Receptor-2, Signaling, Tissue Factor.

ABSTRACT

Cell migration and invasion are very characteristic features of cancer cells that promote metastasis, which is one of the most vulnerable causes of mortality among cancer patients. Emerging evidence has shown that coagulation factors can directly mediate cancer associated complications either by enhancing thrombus formation or by initiating various signaling events leading to metastatic cancer progression. It is well-established that apart from its distinct role in blood coagulation, coagulation factor FVIIa enhances aggressive behaviors of breast cancer cells, but the underlying signaling mechanisms still remain elusive. To this end we investigated FVIIa's role in the migration and invasiveness of the breast cancer cell line MDA-MB-231. Consistent with previous observations, we observed that FVIIa increased the migratory and invasive potential of these cells. We also provide molecular evidence that protease-activated receptor 2 (PAR2) activation, followed by PI3K-AKT activation and GSK3-β inactivation is involved in these processes and that β-catenin a well known tumor regulatory protein, contribute to this signaling pathway. The pivotal role of β-catenin was further indicated by the upregulation of its downstream targets Cyclin D1, c-Myc, COX-2, MMP-7, MMP-14 and Claudin-1. β-catenin knock-down almost completely attenuated the FVIIa-induced enhancement of breast cancer migration and invasion. These findings provide a new perspective to counteract the invasive behavior of breast cancer, indicating that blocking PI3K-AKT pathway-dependent β-catenin accumulation may represent a potential therapeutic approach to control breast cancer.

An increasing body of experimental evidence propose a significant role of Factor VIIa (FVIIa) and Tissue factor (TF) complex in breast cancer progression and metastasis (1). TF, a 47 KDa glycosylated transmembrane protein, is a cellular receptor for plasma clotting Factor VII/VIIa with the primary function of supporting FVII activation and initiating blood coagulation (2–4). TF affects various patho-physiological processes, ranging from embryological development to cancer (5, 6). Previous studies

reveal that TF-deficient mice die due to abnormal fatal bleeding and improper embryonic development (7–9). Though TF-FVIIa induced thrombin generation contributes to some of these patho-physiological processes via activation of platelets, fibrin deposition and activation of protease activated receptor 1 (PAR1)-mediated cell signaling (10), yet it does not account for all TF-dependent processes. Studies so far on TF-FVIIa signaling from several groups have already established the fact that TF-FVIIa binary complex activates PAR2, which is one of the major contributors of tumor growth in breast carcinoma (11–15).

Studies have already established that TF-FVIIa interaction induces migratory ability of various cancer cells including breast cancer (16), whereas the detail signaling mechanism involved still remains elusive. Reports also demonstrate that TF-FVIIa signaling modulates several molecules involved in adhesion, inflammation, proliferation, migration, invasion, and angiogenesis which include β3-integrin, Cyclin D1, Interleukin-1, Survivin and vascular endothelial growth factor in various cancer cells (17). It has also been reported that the pro-metastatic activity of cells is dependent on the extracellular proteolytic activity of FVIIa (17). Studies proclaim that over-expression of TFPI (Tissue Factor Pathway Inhibitor) attenuates the migration of cells by inhibiting TF-FVIIa induced signaling (18). Hence, involvement of TF becomes inevitable in the enhancement of cancer aggressiveness.

β-catenin, a key member in Wnt signaling pathway has also been reported to be involved in multitasking from embryonic development to cancer progression (19). Upon activation of Wnt signaling, β-catenin accumulates in the cells and ultimately regulates differentiation and developmental processes. It also leads to several human diseases of connective tissue, epithelial tissue, bone and cancer including breast cancer (20). Recent reports depict that apart from canonical Wnt signaling, multiple non-canonical pathways also result in cellular accumulation of β-catenin (21).

In this study, we address the accumulation of β-catenin in MDA-MB-231 cells by FVIIa through PAR2 receptor activation followed by PI3K-AKT activation and GSK3β inactivation. TF-FVIIa induced cell signaling promotes transcriptional activation of proteins like Cyclin D1, c-Myc, COX-2, MMP-7, MMP-14 and Claudin-1 directly by manipulating β-catenin transcriptional complex. Interestingly, these proteins have been previously designated as downstream of β-catenin transcriptional complex in Wnt signaling pathway (21). Our findings provide strong evidence that FVIIa-mediated enhanced migration and invasion of MDA-MB-231 cells is guided by β-catenin. These results also provide an insight supportive evidence of a novel signaling mechanism through which a GPCR family protein, PAR2 activation contributes to enhanced aggressiveness of human breast cancer cells and the pathway can be targeted to achieve improved cancer therapeutics to arrest breast tumor growth and increase longevity.

RESULTS

TF-FVIIa interaction leads to β-catenin accumulation in MDA-MB-231 cells- Enhanced migration of cancer cells plays a significant role in cancer metastasis. Among various signaling pathways contributing to the enhancement of migratory potential of cancer cells, Wnt signaling is one of the most prevalent one (20, 22). Growing evidence propose that TF-FVIIa interaction leads to increase in breast cancer cell migration and motility (16). Atypical accumulation of β-catenin has been well studied in various cancerous complications, including breast cancer (23). Up-regulation of cytoplasmic/nuclear β-catenin accumulation has been identified in 40–60% of human breast tumors and is correlated with poor prognosis (24, 25). β-catenin accumulation, due to genetic mutations in Axin, APC or β-catenin as diagnosed in several other tumors, is unusual in breast cancer (26).

These observations suggest that breast cancer cells adapt an alternate or additional mechanism for β-catenin accumulation. As mentioned earlier, the basic mechanism behind breast cancer cell migration due to FVIIa is yet to be elucidated. Hence, to examine the existence of any kind of correlation between these two, we challenged MDA-MB-231, human metastatic breast cancer cells with FVIIa for 5 hrs after 2 hrs of serum deprivation. Interestingly, we observed a consistent time-dependent increase in β-catenin level upto 4 hrs (Fig.1a and b). Our data also indicates an increase in the rate of nuclear β-catenin accumulation in a temporal manner (Fig. 1c and d). Furthermore, semi-quantitative PCR analysis revealed an unaltered mRNA level of β-catenin on subsequent treatment of cells with FVIIa (Fig. 1e and f). Fluorescence microscopic images further confirmed that β-catenin protein accumulates in a significant level inside the cell nucleus at 4 hrs time point after FVIIa exposure (Fig. 1g). Altogether, these findings demonstrate that FVIIa treatment results in β-catenin accumulation in MDA-MB-231 cells without altering its expression level and this leads to β-catenin translocation inside the cell nucleus.

β-catenin accumulation by FVIIa in MDA-MB-231 cells is PAR2 dependent- Previous studies have demonstrated that majority of FVIIa mediated signalings are dependent on PAR2 (27), hence we questioned whether FVIIa modulated β-catenin accumulation in MDA-MB-231 cells is through PAR2 activation or not. To investigate this, we knocked down PAR2 with PAR2 siRNA and treated with FVIIa and PAR2 activation peptide (PAR2AP, a positive control). Efficiency of PAR2 knock-down with PAR2 siRNA was estimated by western blot (Fig. 2a and b). Interestingly, we found complete reversal of FVIIa mediated β-catenin accumulation in PAR2 knocked down cells, strongly establish the involvement of PAR2 in FVIIa-dependant β-catenin accumulation (Fig. 2c and d). Next, we aimed to examine the status of β-catenin in the nucleus of PAR2 activated cells and observed a significant increment of β-catenin inside nucleus (Fig. 2e and f). Here we used Histone H3 as loading control for nuclear lysate and tubulin to measure the purity of nuclear isolation. In consistence with cellular accumulation, we also observed suppressed level of β-catenin accumulation in PAR2 deficient cells after FVIIa treatment (Fig. 2g and h). Fluorescence microscopic images also support less accumulation of β-catenin (red) in cell cytoplasm as well as in nucleus (green) in PAR2-silenced FVIIa challenged cells as compared to the treated ones (yellow nuclei due to green DAPI and red β-catenin co-localization) (Fig. 2i). Intensity quantification of β-catenin was presented in figure 2 (j) for nucleus and figure 2 (k) for cells. As a whole, the findings evidently suggest that PAR2 activation is absolutely required for FVIIa mediated accumulation of β-catenin in MDA-MB-231 cells.

FVIIa induced β-catenin accumulation also occurs in tissue factor and PAR2 over-expressed MCF-7 cells- Here, we examined the involvement of TF in the context of FVIIa-mediated β-catenin accumulation. To analyze the importance of TF, we treated MDA-MB-231 cells with TF-blocking antibody prior to FVIIa addition and observed complete attenuation in β-catenin accumulation (Fig. 3a and b), which confirms that FVIIa-induced β-catenin accumulation is solely TF-dependent. To explore this further, we have used another human breast cancer cell line, MCF-7. We estimated β-catenin accumulation in MCF-7 cells after treatment with FVIIa for 5 hrs and observed no alteration in β-catenin level (Fig. 3c). Interestingly, we found that MCF-7 cells are devoid of any TF and express lower level of PAR2 as compared to MDA-MB-231 (Fig. 3d and e). Therefore, we transfected MCF-7 cells with TF-GFP and PAR2-YFP plasmid constructs, either one or both at a time followed by FVIIa-treatment and cellular β-catenin accumulation was analyzed (Fig. 3f and g). TF over-expressing MCF-7 cells showed increased

levels of cellular β-catenin upon FVIIa treatment. Further elevation in β-catenin accumulation was observed in cells co-transfected with both TF and PAR2 followed by FVIIa treatment. Overall, the data reflect that TF is absolutely needed for FVIIa to cleave PAR2 and induce accumulation of cellular β-catenin. In addition, this result also establishes the fact that PAR2 mediated β-catenin accumulation is not specific for MDA-MB-231 cells but also can take place in other breast cancer cells.

Both TF-FVIIa and PAR2AP modulate β-catenin accumulation in MDA-MB-231 cells via AKT/GSK3β dependent pathway- Glycogen synthase kinase-3β (GSK3β) is a ubiquitously expressed serine/threonine kinase, synchronizes various cellular functions like gene expression, apoptosis, cytoskeletal rearrangement, cell proliferation etc (28). Its activity gets perturbed by phosphorylation, leading to alterations in downstream targets (28). In absence of any upstream stimulus, β-catenin is secluded in an idle state by a multimeric "destruction complex" comprised of GSK3β, Axin and APC (29, 30). APC and Axin act as scaffolding proteins, allowing GSK3β mediated phosphorylation of β-catenin, leading to its ubiquitination and subsequent proteasomal degradation (30). AKT, an upstream regulator of GSK3β has been well reported to play important role in cellular migration and cancer (31). We enquired whether PAR2 activation in MDA-MB-231 cells triggers AKT activation via phosphorylation as well as GSK3β inactivation or not. We noticed that PAR2 activation by TF-FVIIa or PAR2AP leads to increased phosphorylation of both AKT (Thr 308 and Ser 473) and GSK3β (Ser 9) which remain unaffected upon PAR2 knock-down (Fig. 4a, b, c, d, e and f). We also revealed that FVIIa or activation peptide not only causes AKT/GSK3β phosphorylation but also decreases phosphorylation of β-catenin which leads to its subsequent accumulation inside the cell (Fig. 4a and 4b). To further elucidate the importance of AKT, we blocked the PI3K/AKT pathway using two different chemical inhibitors, LY294002 and Wortmanin separately, followed by ligand treatment. As per our anticipation, inhibition of PI3K dramatically reduced the phosphorylation of AKT, GSK3β and increased β-catenin phosphorylation resulting in less β-catenin accumulation due to enhanced degradation of β-catenin (Fig. 4g and h). We further confirmed the involvement of AKT by silencing AKT1 in MDA-MB-231 cells (Fig. 4i) followed by ligand addition (Fig. 4j and k). Results suggest complete reduction of β-catenin accumulation in AKT1 silenced cells. These findings clearly depict that β-catenin accumulation due to PAR2 activation occurs through PI3K/AKT pathway followed by GSK3β inactivation. The nuclear accumulation of β-catenin in the presence/absence of LY294002 in control and PAR2 activated cells was also evident in fluorescent microscopic images (Fig. 5a). Nuclei with DAPI stain (green) revealed no β-catenin accumulation in the nuclei of LY294002 treated or control cells; whereas FVIIa or PAR2AP treated cells with yellow nuclei (due to co-localization of β-catenin and DAPI), indicate significant β-catenin accumulation inside the nucleus. LY294002 addition also reduced nuclear β-catenin accumulation even after FVIIa or PAR2AP treatment. Fig. 5b and c present the intensity of the presence of β-catenin inside the nucleus and cell respectively. Random fields were chosen for imaging and analysis. Number of images taken for every treatment or control analysis was 23,(n=23).

PAR2 activation leads to β-catenin induced transcriptional activation of downstream metastatic proteins- It is well documented that once stabilized, β-catenin translocates to the nucleus and participates in transcriptional activation of responsive genes, critical for tumor cell proliferation and migration via interacting with TCF/LEF (29, 32). In order to study the fate of nuclear translocated β-catenin, TCF/LEF luciferase assay was performed to measure the transcriptional

efficiency of β-catenin. We observed a significant increase of luciferase activity in FVIIa and PAR2AP treated cells (Fig. 6a). This luciferase activity was restrained by introducing PI3K inhibitor (LY294002) (Fig. 6b), which is consistent with our previous observations. To further establish the role of TF and PAR2 in the context of β-catenin mediated transcriptional activation, we over-expressed PAR2-YFP and TF-GFP in MCF-7 cells and performed the TCF-LEF luciferase assay (Fig 6c). We observed that activation of PAR2 also leads to β-catenin accumulation followed by transcriptional activation in MCF-7 cells. Further, we investigated the expression level of downstream responsive genes of β-catenin transcriptional complex. Our semi-quantitative and real time PCR analysis revealed significant rise in the mRNA level of cyclin D1, c-Myc, COX-2, MMP-7, MMP-14 and Claudin-1 during FVIIa and PAR2AP treatment. To distinctively establish the role of β-catenin, we knocked down β-catenin by β-catenin siRNA and observed complete attenuation of these above mentioned transcripts in PAR2 activated cells, indicating the fact that the elevated level of these transcripts by PAR2 activation is guided through β-catenin (Fig. 6d and e). In consistent with the transcriptional status, increase in the protein level of cyclin D1, c-Myc, COX-2, MMP-7, MMP-14 and Claudin-1 was also observed during PAR2 activation which remained unaltered by β-catenin knock-down or by inhibiting PI3K (Fig. 6f and g). These findings clearly indicate that β-catenin translocation inside the nucleus leads to the formation of active β-catenin transcriptional complex which further up-regulates several downstream metastatic proteins.

PAR2 activation promotes migration and invasion of MDA-MB-231 cells through PI3K-AKT dependent β-catenin accumulation- Previous studies have demonstrated that PAR2 mediated signaling induces metastatic behavior of breast cancer both *in vitro* and *in vivo* (17, 33–35). Therefore, to elucidate the signaling molecules involved in this transition, we assessed the metastatic potential by migration (Fig. 7a-d) and invasion assay (Fig. 7e and f). FVIIa and PAR2AP-induced enhancement of MDA-MB-231 cell migration and invasion were perturbed by either inhibiting PI3K or silencing β-catenin, suggesting the active participation of AKT-β-catenin axis in PAR2-dependent cancer metastasis. As a whole, these data clearly demonstrate that PAR2 activation by TF-FVIIa or PAR2AP leads to increased migration and invasion in MDA-MB-231 cells through the interplay of AKT, β-catenin and related molecules.

β-catenin and its downstream members remain well-elevated in human breast cancer tissues as compared to normal breast tissues- So far, ours *in vitro* study indicates that an intrinsic correlation exists between β-catenin accumulation and metastatic potential of breast cancer cells in response to PAR2 activation. Henceforth, to compare the level of β-catenin and its downstream proteins in human breast cancer tissue with respect to normal, samples were collected obeying human ethical regulations. Immunohistochemistry (IHC) data depicts a significant level of β-catenin accumulation in cancer tissue as compare to normal (Fig. 8a). In consistent with IHC, western blot data also revealed an elevated level of β-catenin and its downstream members in breast cancer tissue (Fig. 8b). Interestingly, we also observed considerable increment of TF level in tumor tissue samples. To further analyze the expression profile of β-catenin downstream members, we have also performed the real time PCR analysis of mRNA isolated from cancer and normal breast tissues (Fig. 8c). In consistent with our previous observations, we also found an up-regulation of β-catenin target gene expressions at mRNA level. In conclusion, the enhanced pattern of the signature molecules in cancer tissue was observed similar to ours *in vitro* analysis, suggesting the active involvement of similar pathway in operation in both the *in vivo* and *in vitro* conditions.

DISCUSSION

Apart from blood coagulation, the role of coagulation proteases in cancer progression has been well established (36). Evidence exist that the primary initiator of the main coagulation cascade, TF is also involved in oncogenic progression, precisely tumor metastasis and angiogenesis (16). Through *in vitro* studies, the contribution of coagulation proteases TF-FVIIa and its correlation with various cellular signaling pathways have been well accepted as a tumor promoter (35, 37, 38). Most human epithelial cancers have high levels of TF and PAR2 (39, 40). Though the distinct *in vivo* contribution of TF is well-documented, but the role of its only ligand FVIIa remains elusive due to distant possibility of its proximity with extra-vascular cells (where TF physically resides) after crossing endothelial barrier. Identification of Endothelial Protein C Receptor (EPCR) as an auxiliary receptor for FVIIa (41) and its transcytosis by EPCR provides a novel mechanism for the transfer of FVIIa from blood flow to extra vascular tissues, crossing the endothelial barrier. Its redistribution to extra-vascular tissues with prolonged retention, paved the way for accepting FVIIa as an active *in vivo* PAR2 activator through TF (42).

Several studies regarding breast cancer have portrayed TF-FVIIa as an active inducer of cancer cell migration, invasion and proliferation. But the details of the signaling mechanisms leading to this progression are still unexplored. Through this approach we have addressed the molecular events responsible for the aggressiveness of breast cancer cells in response to FVIIa. In this study, the observed β-catenin accumulation by FVIIa via AKT pathway appears to be a novel mechanism by which PAR2 contributes to breast cancer cell migration and invasion. Our results support a pivotal role of PAR2 activation in promoting metastatic behavior of breast cancer cells. The eloquent mechanism that we disambiguate to report this important function of PAR2 activation is that it increases β-catenin stabilization and subsequent nuclear translocation. Furthermore, we showed that PAR2 activation-dependent stabilization of β-catenin is acquired by coordinating the activation of AKT/GSK3β signaling leading to destruction of β-catenin phosphorylation complex (Fig. 9). We also provide molecular evidence supporting the regulatory role of PAR2 and AKT in β-catenin stabilization, and its nuclear translocation. The significance of our *in vitro* result is strengthened by the fact that the key component β-catenin of this pathway is well detected in elevated levels in human breast tumors.

The dual functioning molecule β-catenin intensifies cell-cell adhesion when bound to E-cadherin complexes and also performs a transcriptional co-activator role after nuclear translocation (43). Deprivation of E-cadherin-β-catenin complex and nuclear translocation of β-catenin are vital for the development of migratory characteristics of cancer cells (29, 44, 45). These findings suggest that PAR2 activation promotes nuclear translocation of β-catenin and increases the recruitment of β-catenin at TCF/LEF-binding sites. PAR2AP induces overactive β-catenin signaling which leads to enhanced co-activation function as evident by higher levels of TCF/LEF-responsive genes (like Cyclin D1, c-Myc etc.). Up-regulation of cyclin D1 has been implicated in acquisition of higher proliferative effect (46–48). Nuclear β-catenin induces tumor invasion supporting genes and transition to metastatic phenotype via recruiting the transcriptional co-activators and cyclic AMP response element binding protein (21). In absence of enzymatic activities, β-catenin has been considered as "non targetable". Whereas, recent findings show that other aspects of this pathway such as β-catenin stabilization or transcriptional activities can be aimed to inhibit its downstream effects. We speculated that disruption of the β-catenin mediated transcriptional complex assembly could be a productive strategy to inhibit PAR2 activation induced cell migratory and invasive property. Consistent knock-down of β-

catenin or PI3K inhibition completely attenuates PAR2 mediated metastatic potential of breast cancer cells. Hence, targeting PAR2 activation-induced hyperactive β-catenin signaling with small molecule inhibitors could represent a novel and effective strategy for therapeutic intervention. We showed that perturbing PAR2 receptor dramatically reduces the phosphorylation of GSK3β. Blocking of GSK3β inhibition can also be a potential target for therapeutic approach alongside conventional chemo/radiation therapy against breast cancer progression.

MATERIALS AND METHODS

Cell Culture- The human breast cancer cell lines MCF-7 and MDA-MB-231 were obtained from the American Type Culture Collection and were cultured in standard DMEM (Gibco) supplemented with 10% FBS and penicillin-streptomycin (100 U/ml) (Invitrogen). Cells were maintained in a humidified chamber at 37˚C and 5% CO_2 level. Cells were seeded on 12-well plates at a density of 0.1 X 10^6 and allowed to grow to confluence. Serum starvation was given for 2 hours followed by treatment with human recombinant Factor VIIa (Novo Nordisk) (100 nM) and PAR2 activation peptide (SLIGKV-NH_2; 100 μM) (GLBiochem, China). In other set of experiments, cells were treated with PI3K-inhibitor LY294002 (20μM; Calbiochem) and Wortmanin (50 μM; Sigma). Antibodies against β-catenin, Tissue Factor and PAR2 from Abcam, GAPDH and Histone H3 from sigma, p-AKT, AKT, p-GSK3β, GSK3β, Cyclin D1, c-Myc, COX2, MMP-7, MMP-14, Claudin-1 and Tubulin antibodies from Cell Signaling Technology were purchased and used at a dilution of instruction manual. HRP-conjugated anti-rabbit and anti-mouse secondary antibodies were obtained from Sigma.

Transfection of Plasmid Constructs- TF-GFP and PAR2-YFP constructs were transfected into MCF-7 cells by using lipofectamine 2000 (Invitrogen) following manufacturer's protocol.

Western Blotting (WB)- Cells were lysed with laemmli buffer after definite time point of ligands treatment. The lysate was subjected to heat at 95ºC for 5 minutes. Proteins were separated by SDS-PAGE and transferred onto PVDF membrane which was blocked in 5% non-fat dried milk in TBS and incubated overnight at 4°C with primary antibodies in 3% BSA/TBS for specific proteins. After washing with TBS-T (TBS, 1% Tween20), secondary antibody incubation was given for an hour followed by washing and development by ECL method. Densitometry of the blot was performed by image J and graphs were prepared by GraphPad Prism 5.

Tissue Factor Blocking Experiment- MDA-MB-231 cells were seeded in 12-well plates and allowed to grow to full confluency. Cell monolayer was incubated at room temperature for 2 hrs with TF polyclonal blocking antibody which binds to TF receptors of cell surface, followed by treatment with FVIIa for 4 hrs. Cells were lysed thereafter by Laemmli buffer and WB analysis was performed to check β-catenin accumulation level.

Preparation of Subcellular Fractions- Equal number of MDA-MB-231 cells were seeded in 35 mm dish and allowed to attain 100% confluency. After 2 hrs of serum starvation, cells were treated with FVIIa and PAR2 agonist peptide for 4 hrs. Cytoplasmic and nuclear fractions were prepared by incubating the cells in 50 μl of ice cold lysis buffer [10 mM NaCl, 10 mM Tris-HCl (pH 7.4), 3 mM $MgCl_2$, 0.5% Nonidet P40, 0.1 mM PMSF and protease inhibitor cocktail]. Lysate was kept for 7-8 mins on ice followed by centrifugation at 8000g for 15 mins at 4ºC to precipitate nuclei. Supernatant was stored as a cytoplasmic fraction. Nuclear pellet was incubated in 50 μl chilled nuclear extraction buffer [20 mM Tris-HCl (pH=7.9), 0.42 M KCl, 0.2 mM EDTA, 10% glycerol, 2 mM DTT, 0.1 mM

PMSF and protease inhibitor cocktail] for 20 mins followed by centrifugation at 21,000 g for 15 mins at 4ºC to precipitate the nuclear debris. Equal volume of lysate was subjected to western blot analysis.

Immunofluorescence - Cells were seeded onto cover slips etched in 35% HF for 10 secs. Cells were serum starved for 2 hrs and treated with FVIIa and PAR2 activation peptide for 4 hrs followed by washing with PBS and fixing with 4% PFA for 30 mins. Cells were permeabilized with 0.1% Triton X-100 for 10 mins and then blocked with 5% BSA, an hour after washing it thrice with PBS. Cells were incubated with β-catenin primary antibody overnight at and after washing were treated with Alexa-fluor 555-rabbit secondary antibody for 1 hr. After washing, the slides were exposed to DAPI for 10-20 mins and again washed with PBS. Cells were imaged with the sCMOS camera (Orca Flash 4.0, Hamamatsu) on an inverted fluorescence microscope from Carl Zeiss (Axio-observer Z1).

Image analysis- Cell images were taken with 63X magnification (N.A 1.4) using Carl Ziess axio observer Z1 microscope. Images were analyzed using imageJ software. Calculations were performed using MATLAB.

β-Catenin-TCF/LEF regulated reporter gene assay- MDA cells were seeded in T-25 at a seeding density of $0.7x10^6$ cells and incubated to grow for 24 hrs. On the following day, cells were transfected with 4µgm of either a β-catenin-TCF/LEF sensitive or insensitive reporter vector (TOP FLASH/FOP FLASH) (Upstate Biotechnology Inc), using Lipofectamine 2000 reagent (Invitrogen) according to manufacturer's instructions. Next day, cells were trypsinised, washed with serum free medium, counted and seeded at 40,000 cells per well in 96 well plate. Subsequently with cell adherence, after 2 hrs of serum starvation PI3k inhibitor was added to the medium at required concentration before 1 hr of FVIIa or PAR2AP treatment with LiCl as positive control. After 6 hrs of treatment, cells were analysed for luciferase activity using the Steady – Glo Luciferase assay system (Promega) according to instruction manual.

Migration Assay- Equal number of MDA-MB-231 cells were seeded onto 35-mm dishes and allowed to reach 60-70% confluency. Cells were transfected with β-catenin or PAR2-siRNA (100 nM) by using Lipofectamine 2000 (Invitrogen) and incubated for 48 hrs. On the day of experiment, single scratch-lines of equal width were made using a micro tip. Both knocked-down and untreated cells were serum starved for 2 hrs followed by treatment with FVIIa or PAR2AP. LY294002 (PI3K pathway inhibitor) was added 1 hr prior to ligands treatment. After 36 hrs, images were taken and number of cells migrated to the scratched area was estimated. Migratory potential of the cells were evaluated by comparing with 0 hr treatment.

Invasion Assay- MDA-MB-231 cells were grown in T25 flask and β-catenin knock-down was performed. Equal number of control and knocked-down cells were seeded on the matrigel (Sigma)-coated upper compartment of a transwell chamber in serum-free media. FVIIa or PAR2AP treatment was done and LY294001 was added 1 hr before ligands addition. FBS containing DMEM was placed in the lower compartment, and further incubation was carried out for 24 hrs. Extravasated cells to the lower surface of the membrane were stained with crystal violet solution after scraping off the upper surface cells. Total number of invaded cells was counted in 10 randomly selected fields under a bright-field microscope and a comparative graphical analysis was done using GraphPad Prism 5 after repeating the experiments thrice.

Gene knockdown of β-catenin, PAR2 and AKT1 by siRNA- Transfection of siRNA against human β-catenin, PAR2 and AKT1 and non target siRNAs into cells was performed at a concentration of 100

nM using Lipofectamine 2000 as per manufacturer's guidelines. Their respective sequences are as follows: β-catenin siRNA 5'-GUUAUGGUCCAUCAGCUUU-3', PAR2 siRNA1-5'-CUUUGUAUGUCGUGA AGCA-3', PAR2 siRNA2- 5'-AGUCGUGAAUCUUGUUCAATT-3', PAR2 scrambled siRNA 5'-GGACUCUUUAUGGUACGUUUAGAUU-3' and AKT 1 siRNA1- 5'-CAG CCC UGA AGU ACU CUU U-3', AKT 1 siRNA2-5' GGA CGG GCA CAT TAA GAT CTT 3', scrambled siRNA 5'-AGGUAGUGUAAUCGCCUUGUUTT -3'

Reverse transcription and quantitative PCR- Extraction of total cellular RNA was performed using TRIZOL reagent (Life Technologies, USA). The extracted RNA was used for reverse transcription with the Super-Script III First-Strand cDNA Synthesis System (Invitrogen) according to the manufacturer's protocol. The cDNA was used for qRT-PCR with SYBR Green Master Mix (Applied Biosystems, USA) on the Step One plus Real-Time PCR System (Applied Biosystems). All values were normalized with GAPDH. Primer sequences for Real Time PCR are Cyclin D1 forward primer 5'-ACAAACAGATCATCCGCAAACAC-3' and reverse primer 5'-TGTTGGGGCTCCTCAGGTTC-3', c-Myc forward primer 5'-AAACACAAACTTGAACAGCTAC-3' and reverse primer 5'-ATTTGAGGCAGTTTACATTATGG-3', COX-2 forward primer 5'-TCAAATGAGATTGTGGAAAAAT-3' and reverse primer 5'-AGATCATCTCTGCCTGAGTATCTT-3', MMP7 forward 5′-TGAGCTACAGTGGGAACAGG-3′; and reverse, 5′-TCATCGAAGTGAGCATCTCC-3′, MMP14 forward primer 5'-TTGGACTGTCAGGAATGAGG-3' and 5'-GCAGCACAAAATTCTCCGTG-3', Claudin1 forward primer 5'-TCTACGAGGGACTGTGGATG-3', reverse primer 5'-TCAGATTCAGCTAGGAGTCG-3' and GAPDH forward 5'-AACGGGAAGCCCATCACC-3'; reverse 5'-CAGCCTTGGCAGCACCAG-3'.

Immunohistochemistry– Breast tumor and normal breast tissues (n=10 for each, normal and tumor) were obtained from Netaji Subhash Chandra Bose Cancer Research Institute, Kolkata following proper norms of human ethics. Working protocols with tissue samples were also approved by human ethics committee of Netaji Subhash Chandra Bose Cancer Research Institute, Kolkata (Reg.No. ECR/286/INST/WB/2013) and all the samples were collected obeying the human ethics committee rules. Both cancer and normal tissues were de-paraffinized in xylene and dehydrated through various concentrations of ethanol and again rehydrated. The sections were incubated in wash buffer (0.05M TBS with 0.01% Tween-20) for 5 mins. Heat-induced epitope retrieval was performed in 10mM citrate buffer (pH 6.0) in a microwave for two sessions of 5 mins. After blocking with 3% H_2O_2 for 10-12 mins, the treated tissue slides were rinsed gently with wash buffer and then incubated with β-catenin primary antibody at 4°C overnight at 1:100 dilutions. Tissue slides were washed with TBS and subsequently incubated with HRP-conjugated secondary. Again after subsequent washes the slides were treated with DAB and H_2O_2 mix followed by counterstaining with haematoxylin. Separate slides for haematoxylin and eosins are also prepared.

Statistical analysis- The images of western blot and other techniques are representative of at least three independent experiments. The data presented over here are as mean ±S.E of the mean. Differences are considered to be statistically significant at $p < 0.05$ using student's t-test.

Acknowledgement

This project work was supported by the fund provided by the DST project grant (DST No-SR/SO/BB-0125/2012) from Department of Science and Technology, Govt. of India and startup grant of IACS. Authors thank the instrument facilities provided from Department of Biological Chemistry, Indian Association for the Cultivation of Science, Kolkata. We pay our gratitude to Dr. Sanghamitra Raha of SINP, Kolkata for providing different constructs including TCF/LEF Luciferase constructs, many antibodies and the reagents for our work. We are thankful to the staff of Netaji Subhash Cancer Research Institute, Kolkata for their humble co-operation and effort in providing breast cancer tissue samples for the study.

Conflict of interest: All authors declare that they have no conflicts of interest with the contents of this article.

Author Contributions: A.R. and P.S. designed the project; A.R. and S.A. performed the research work and analyzed data; A.B. cloned TF and PAR2 constructs. K.D., R.P. and S.M. assisted in the experiments. A.M. provided tissue sample for research, A.R. and P.S. wrote the manuscript.

REFERENCES

1. Versteeg, H. H., and Spek, C. A. (2003) C HAPTER 6 The Pleiotropic Effects of Tissue Factor Linking TF-Associated Physiology to Intracellular Signaling

2. Sabharwal, A. K., Birktoft, J. J., Gorka, J., Wildgoose, P., Petersen, L. C., and Bajaj, S. P. (1995) High affinity Ca(2+)-binding site in the serine protease domain of human factor VIIa and its role in tissue factor binding and development of catalytic activity. *J. Biol. Chem.* **270**, 15523–30

3. Mann, K. G. (1999) Biochemistry and physiology of blood coagulation. *Thromb. Haemost.* **82**, 165–74

4. Prasad, R., and Sen, P. (2017) Structural modulation of factor VIIa by full-length tissue factor (TF_{1-263}): implication of novel interactions between EGF2 domain and TF. *J. Biomol. Struct. Dyn.* 10.1080/07391102.2017.1289125

5. Cole, M., and Bromberg, M. (2013) Tissue factor as a novel target for treatment of breast cancer. *Oncologist*. **18**, 14–8

6. Carmeliet, P., Mackman, N., Moons, L., Luther, T., Gressens, P., Van Vlaenderen, L., Demunck, H., Kasper, M., Breier, G., Evrard, P., Müller, M., Risau, W., Edgington, T., and Collen, D. (1996) Role of tissue factor in embryonic blood vessel development. *Nature*. **383**, 73–75

7. Toomey, J., Kratzer, K., Lasky, N., Stanton, J., and Broze, G. J. (1996) Targeted disruption of the murine tissue factor gene results in embryonic lethality. *Blood*. **88**, 1583–1587

8. Bugge, T. H., Xiao, Q., Kombrinck, K. W., Flick, M. J., Holmbäck, K., Danton, M. J., Colbert, M. C., Witte, D. P., Fujikawa, K., Davie, E. W., and Degen, J. L. (1996) Fatal embryonic bleeding events in mice lacking tissue factor, the cell-associated initiator of blood coagulation. *Proc. Natl. Acad. Sci. U. S. A.* **93**, 6258–63

9. Rosen, E. D., Chan, J. C., Idusogie, E., Clotman, F., Vlasuk, G., Luther, T., Jalbert, L. R.,

Albrecht, S., Zhong, L., Lissens, A., Schoonjans, L., Moons, L., Collen, D., Castellino, F. J., and Carmeliet, P. (1997) Mice lacking factor VII develop normally but suffer fatal perinatal bleeding. *Nature*. **390**, 290–4

10. Ruf, W., and Mueller, B. (2006) Thrombin Generation and the Pathogenesis of Cancer. *Semin. Thromb. Hemost.* **32**, 061–068

11. Morris, D. R., Ding, Y., Ricks, T. K., Gullapalli, A., Wolfe, B. L., and Trejo, J. (2006) Protease-activated receptor-2 is essential for factor VIIa and Xa-induced signaling, migration, and invasion of breast cancer cells. *Cancer Res.* **66**, 307–14

12. Schaffner, F., and Ruf, W. (2008) Tissue factor and protease-activated receptor signaling in cancer. *Semin. Thromb. Hemost.* **34**, 147–53

13. Versteeg, H. H., Borensztajn, K. S., Kerver, M. E., Ruf, W., Reitsma, P. H., Spek, C. a, and Peppelenbosch, M. P. (2008) TF:FVIIa-specific activation of CREB upregulates proapoptotic proteins via protease-activated receptor-2. *J. Thromb. Haemost.* **6**, 1550–7

14. Versteeg, H. H., Schaffner, F., Kerver, M., Petersen, H. H., Ahamed, J., Felding-Habermann, B., Takada, Y., Mueller, B. M., and Ruf, W. (2008) Inhibition of tissue factor signaling suppresses tumor growth. *Blood*. **111**, 190–9

15. Versteeg, H. H., Schaffner, F., Kerver, M., Ellies, L. G., Andrade-Gordon, P., Mueller, B. M., and Ruf, W. (2008) Protease-activated receptor (PAR) 2, but not PAR1, signaling promotes the development of mammary adenocarcinoma in polyoma middle T mice. *Cancer Res.* **68**, 7219–27

16. Hjortoe, G. M., Petersen, L. C., Albrektsen, T., Sorensen, B. B., Norby, P. L., Mandal, S. K., Pendurthi, U. R., and Rao, L. V. M. (2004) Tissue factor-factor VIIa-specific up-regulation of IL-8 expression in MDA-MB-231 cells is mediated by PAR-2 and results in increased cell migration. *Blood*. **103**, 3029–37

17. Bluff, J. E., Brown, N. J., Reed, M. W. R., and Staton, C. A. (2008) Tissue factor, angiogenesis and tumour progression. *Breast Cancer Res.* **10**, 204

18. Stavik, B., Skretting, G., Aasheim, H.-C., Tinholt, M., Zernichow, L., Sletten, M., Sandset, P. M., and Iversen, N. (2011) Downregulation of TFPI in breast cancer cells induces tyrosine phosphorylation signaling and increases metastatic growth by stimulating cell motility. *BMC Cancer*. **11**, 357

19. Huang, H., and He, X. (2008) Wnt/β-catenin signaling: new (and old) players and new insights. *Curr. Opin. Cell Biol.* **20**, 119–125

20. Clevers, H., and Nusse, R. (2012) Wnt/β-catenin signaling and disease. *Cell*. **149**, 1192–205

21. Rao, T. P., and Kühl, M. (2010) An updated overview on Wnt signaling pathways: a prelude for more. *Circ. Res.* **106**, 1798–806

22. Anastas, J. N., and Moon, R. T. (2013) WNT signalling pathways as therapeutic targets in cancer. *Nat. Rev. Cancer*. **13**, 11–26

23. Brennan, K. R., and Brown, A. M. C. (2004) Wnt proteins in mammary development and cancer. *J. Mammary Gland Biol. Neoplasia*. **9**, 119–31

24. Lin, S. Y., Xia, W., Wang, J. C., Kwong, K. Y., Spohn, B., Wen, Y., Pestell, R. G., and Hung, M.

C. (2000) Beta-catenin, a novel prognostic marker for breast cancer: its roles in cyclin D1 expression and cancer progression. *Proc. Natl. Acad. Sci. U. S. A.* **97**, 4262–6

25. Nakopoulou, L., Mylona, E., Papadaki, I., Kavantzas, N., Giannopoulou, I., Markaki, S., and Keramopoulos, A. (2006) Study of phospho-β-catenin subcellular distribution in invasive breast carcinomas in relation to their phenotype and the clinical outcome. *Mod. Pathol.* **19**, 556–563

26. Candidus, S., Bischoff, P., Becker, K. F., and Höfler, H. (1996) No evidence for mutations in the alpha- and beta-catenin genes in human gastric and breast carcinomas. *Cancer Res.* **56**, 49–52

27. Camerer, E., Huang, W., and Coughlin, S. R. (2000) Tissue factor- and factor X-dependent activation of protease-activated receptor 2 by factor VIIa. *Proc. Natl. Acad. Sci. U. S. A.* **97**, 5255–60

28. Jope, R. S., and Johnson, G. V. W. (2004) The glamour and gloom of glycogen synthase kinase-3. *Trends Biochem. Sci.* **29**, 95–102

29. Moon, R. T., Bowerman, B., Boutros, M., and Perrimon, N. (2002) The promise and perils of Wnt signaling through beta-catenin. *Science*. **296**, 1644–6

30. Kimelman, D., and Xu, W. (2006) Beta-Catenin Destruction Complex: Insights and Questions From a Structural Perspective. *Oncogene*. **25**, 7482–91

31. Åberg, M., and Siegbahn, A. (2013) Tissue factor non-coagulant signaling - molecular mechanisms and biological consequences with a focus on cell migration and apoptosis. *J. Thromb. Haemost.* **11**, 817–25

32. Micalizzi, D. S., Farabaugh, S. M., and Ford, H. L. (2010) Epithelial-mesenchymal transition in cancer: parallels between normal development and tumor progression. *J. Mammary Gland Biol. Neoplasia*. **15**, 117–34

33. Versteeg, H. H., Spek, C. A., Peppelenbosch, M. P., and Richel, D. J. (2004) Tissue factor and cancer metastasis: the role of intracellular and extracellular signaling pathways. *Mol. Med.* **10**, 6–11

34. Steinhoff, M., Buddenkotte, J., Shpacovitch, V., Rattenholl, A., Moormann, C., Vergnolle, N., Luger, T. a, and Hollenberg, M. D. (2005) Proteinase-activated receptors: transducers of proteinase-mediated signaling in inflammation and immune response. *Endocr. Rev.* **26**, 1–43

35. Kocatürk, B., and Versteeg, H. H. (2013) Tissue factor-integrin interactions in cancer and thrombosis: every Jack has his Jill. *J. Thromb. Haemost.* **11 Suppl 1**, 285–93

36. Lima, L. G., and Monteiro, R. Q. (2013) Activation of blood coagulation in cancer: implications for tumour progression. *Biosci. Rep.* 10.1042/BSR20130057

37. Degen, J. L., and Palumbo, J. S. (2012) Hemostatic factors, innate immunity and malignancy. *Thromb. Res.* **129**, S1–S5

38. Sallah, S., Wan, J. Y., Nguyen, N. P., Hanrahan, L. R., and Sigounas, G. (2001) Disseminated intravascular coagulation in solid tumors: clinical and pathologic study. *Thromb. Haemost.* **86**, 828–33

39. van den Berg, Y. W., Osanto, S., Reitsma, P. H., and Versteeg, H. H. (2012) The relationship between tissue factor and cancer progression: insights from bench and bedside. *Blood*. **119**, 924–

932

40. Su, S., Li, Y., Luo, Y., Sheng, Y., Su, Y., Padia, R. N., Pan, Z. K., Dong, Z., and Huang, S. (2009) Proteinase-activated receptor 2 expression in breast cancer and its role in breast cancer cell migration. *Oncogene*. **28**, 3047–57

41. Sen, P., Clark, C. A., Gopalakrishnan, R., Hedner, U., Esmon, C. T., Pendurthi, U. R., and Vijaya Mohan Rao, L. (2012) Factor VIIa binding to endothelial cell protein C receptor: Differences between mouse and human systems. *Thromb. Haemost.* **107**, 951–961

42. Nayak, R. C., Sen, P., Ghosh, S., Gopalakrishnan, R., Esmon, C. T., Pendurthi, U. R., and Rao, L. V. M. (2009) Endothelial cell protein C receptor cellular localization and trafficking: Potential functional implications. *Blood*. **114**, 1974–1986

43. Cadigan, K. M., and Liu, Y. I. (2006) Wnt signaling: complexity at the surface. *J. Cell Sci.* **119**, 395–402

44. Yan, D., Avtanski, D., Saxena, N. K., and Sharma, D. (2012) Leptin-induced epithelial-mesenchymal transition in breast cancer cells requires β-catenin activation via Akt/GSK3- and MTA1/Wnt1 protein-dependent pathways. *J. Biol. Chem.* **287**, 8598–612

45. Tian, X., Liu, Z., Niu, B., Zhang, J., Tan, T. K., Lee, S. R., Zhao, Y., Harris, D. C. H., and Zheng, G. (2011) E-cadherin/β-catenin complex and the epithelial barrier. *J. Biomed. Biotechnol.* **2011**, 567305

46. Yang, K., Hitomi, M., and Stacey, D. W. (2006) Variations in cyclin D1 levels through the cell cycle determine the proliferative fate of a cell. *Cell Div.* **1**, 32

47. Yu, Q., Geng, Y., and Sicinski, P. (2001) Speci ® c protection against breast cancers by cyclin D1 ablation

48. Fredersdorf, S., Burns, J., Milne, A. M., Packham, G., Fallis, L., Gillett, C. E., Royds, J. A., Peston, D., Hall, P. A., Hanby, A. M., Barnes, D. M., Shousha, S., O'Hare, M. J., and Lu, X. (1997) High level expression of p27(kip1) and cyclin D1 in some human breast cancer cells: inverse correlation between the expression of p27(kip1) and degree of malignancy in human breast and colorectal cancers. *Proc. Natl. Acad. Sci. U. S. A.* **94**, 6380–5

FOOTNOTES

This work was supported by project grants from Department of Science and Technology, Govt. of India (DST No- SR/SO/BB-0125/2012) and IACS Kolkata.

The abbreviations used are: FVIIa, Factor VIIa; PAR2, Protease Activated Receptor 2; PAR2AP, Protease Activated Receptor 2 Agonist Peptide; TF, Tissue Factor; PI3K, Phosphatidyl Inositol-3-Kinase.

Figure Legends

Figure 1. **Accumulation of β-catenin in MDA-MB-231 cells due to FVIIa treatment.** Cells were seeded onto 12-well plate and allowed to grow. After 2 hrs serum starvation cells were treated with FVIIa (100 nM). (a) Time-dependent accumulation of β-Catenin was estimated by standard western blotting protocol taking GAPDH as a loading control. (b) Band intensity was measured and quantified using ImageJ and graph was plotted by GraphPad Prism 5. (c) Nuclear accumulation of β-Catenin was analyzed by western blotting of nuclear lysate with Histone H3 as loading control. LiCl was used as a positive control. Tubulin was used as a measure of nucleus isolation purity. (d) Quantification of nuclear translocated β-Catenin was done by ImageJ and graph was plotted by using GraphPad Prism 5. (e) Semi-quantitative PCR analysis was performed for checking the expression status of β-Catenin gene in the cells after treatment with FVIIa for various time points. (f) Quantitative estimation of β-Catenin band intensity over GAPDH was done by using ImageJ and GraphPad Prism 5. The images of western blot and RT-PCR analysis are representative of at least three independent experiments. The data presented over here are as mean ±S.E. of the mean. Differences are considered to be statistically significant at $p < 0.05$ using student's t-test. (g) Cells were grown onto cover-glasses followed by treatment with FVIIa. Cells were fixed with 4% PFA and permeabilized with 0.01% Triton-X-100 followed by immunostaining with β-Catenin antibody and DAPI was used for staining nucleus, scale bar = 25μm. Quantitative estimation of β-Catenin inside the cells and nucleus was performed by ImageJ and MATLAB software, number of samples(n) per treatment were 23. Graphical representation of β-Catenin intensity in nucleus were presented in figure (h) and intensity in cells in figure (i).

Figure 2. **β-catenin accumulation by FVIIa in MDA-MB-231 cells occurs through PAR2 activation.** MDA-MB-231 cells were transfected with PAR2 siRNA1, 2 using Lipofectamine 2000 along with a scrambled siRNA as control and allowed to grow for 48 hrs. (a) PAR2 knock-down was verified by western blotting. (b) Quantitative estimation of PAR2 band intensity over GAPDH was done by using ImageJ and GraphPad Prism 5. (c) Untreated, scrambled siRNA and PAR2 siRNA1 treated cells were serum starved for 2 hrs and stimulated with FVIIa and PAR2AP (10 μM) and the accumulation of β-Catenin was measured after 4 hrs by western blotting. (d) Band intensity of β-Catenin over GAPDH was estimated by using ImageJ and GraphPad Prism 5. (e) β-Catenin accumulation at nuclear level upon treating the cells with PAR2AP. (f) Quantification of nuclear β-Catenin was done by ImageJ and GraphPad Prism 5. (g) Nuclear accumulation of β-Catenin was verified in PAR2 silenced and control scrambled siRNA treated cells after challenging with FVIIa. (h) Quantitative analysis of nuclear β-Catenin over Histone H3 was performed by using ImageJ and GraphPad Prism 5. All the experiments were performed at least for three times and the data denoted as mean ±S.E. of the mean. Differences are statistically significant at $p < 0.05$ using student's t-test. (i) Cells were transfected with PAR2 siRNA followed by treatment with FVIIa and PAR2AP. β-Catenin accumulation was analyzed by immunostaining with β-Catenin antibody. Nucleus was stained with DAPI, scale bar = 25 μm. Quantitative estimation of β-Catenin inside the cells and nucleus was performed by ImageJ and MATLAB software, number of samples(n) per treatment were 23. Graphical representation of β-Catenin intensity in nucleus were presented in figure (j) and intensity in cells in figure (k).

Figure 3. **Involvement of tissue factor in FVIIa-induced accumulation of β-catenin.** (a) MDA-MB-231 cells were treated with TF-blocking antibody for 2 hrs followed by challenging with FVIIa, and β-Catenin accumulation was analyzed after 4 hrs by western blot analysis. (b) Quantification of β-Catenin accumulation was performed by using ImageJ and GraphPad Prism 5. (c) Quantitative estimation of β-Catenin accumulation by western blotting was checked in MCF-7 cells upon treatment with FVIIa at various time intervals (0-5 hrs). (d) Relative level of TF and PAR2 was measured in MCF-7 and MDA-MB-231 cells by western blot. (e) Relative PAR2 band intensity was quantified over GAPDH in MCF-7 and MDA-MB-231 cells by ImageJ and GraphPad Prism 5. (f) TF, PAR2 and β-Catenin levels in control, TF-GFP and PAR2-YFP over-expressed MCF-7 cells were analyzed by western blot after FVIIa or PAR2AP treatment. (g) Band intensity of β-Catenin over GAPDH in control, TF-GFP and PAR2-YFP over-expressed MCF-7 cells was quantified by using ImageJ and GraphPad Prism 5. All the experiments were performed at least thrice and data presented as mean ±S.E. of the mean. The differences are considered to be statistically significant at $p < 0.05$ using student's t-test.

Figure 4. **TF-FVIIa or PAR2AP modulate β-catenin accumulation in MDA-MB-231 cells via AKT/GSK3β dependent pathway.** (a) AKT (both at Thr 308 and Ser 473), 10 mins, (b) Cells were challenged with FVIIa, PAR2AP along with a positive control LiCl (40 mM) and the phosphorylation status of GSK3β (at Ser 9), β-Catenin and phospho-β-Catenin levels were checked at 1 , 4 and 4 hrs, respectively by western blotting. (c) Phospho-AKT (at Thr 308 and Ser 473) and GSK3β (at Ser 9) were checked in PAR2 siRNA1 and scrambled siRNA treated cells after challenging with FVIIa. (d), (e) and (f) Quantitative band intensity of phospho-AKT at Thr 308, Ser 473 and phospho-GSK3β at Ser 9 normalized by respective proteins were measured by using ImageJ and GraphPad Prism 5. Cells were treated with either (g) LY294002 (20 μM) or (h) Wortmanin (50 μM) 1 hr before FVIIa or PAR2AP treatment and the cell lysate were analyzed for phospho-AKT (both at Thr 308 and Ser 473), GSK3β (at Ser 9), β-Catenin and phospho-β-Catenin by western blot. (i) AKT 1 knock-down was performed by two siRNAs (1, 2) and analyzed by western blotting. (j) β-Catenin levels were estimated in scrambled and AKT 1 knock-down cells after FVIIa treatment by western blotting. (k) Accumulated β-Catenin levels (normalized by GAPDH) were quantified by ImageJ and GraphPad Prism 5. All the experiments were performed at least for three times. The data presented here are as mean ±S.E. of the mean. The differences are considered to be statistically significant at $p < 0.05$ using student's t-test.

Figure 5. **β-Catenin accumulation was assessed by fluorescence microscopy upon inhibiting PI3K with LY294002 followed by PAR2 activation.** (a) Cells were treated with LY294002 followed by treatment with FVIIa and PAR2AP. β-Catenin accumulation was analyzed by immunostaining with β-Catenin antibody. Nucleus was stained with DAPI, scale bar = 25 μm. Quantitative estimation of β-Catenin inside the cells and nucleus was performed by ImageJ and MATLAB software, number of samples(n) per treatment were 23. Graphical representation of β-Catenin intensity in nucleus were presented in figure (b) and intensity in cells in figure (c).

Figure 6. **PAR2 activation leads to β-catenin induced transcriptional activation of downstream proteins.** (a) MDA-MB-231 cells, transfected with TCF/LEF sensitive or insensitive reporter vector were seeded in 96-well plate with full confluency and subjected to 2 hrs serum starvation followed by FVIIa, PAR2AP and LiCl (used as a positive control) treatment for 6 hrs. Luciferase activity of the cell lysates were analysed using the Steady-Glo Luciferase assay system and graph was plotted using GraphPad Prism 5. (b) Similarly, luciferase activity was quantified for LY294002-pretreated FVIIa/PAR2AP challenged cells. (c) Like MDA-MB-231 cells, normal MCF-7, TF-GFP and/or PAR2-YFP over-expressed MCF-7 cells were transfected with TCF/LEF sensitive or insensitive reporter vector and relative luciferase activity was measured after treatment with FVIIa or PAR2AP, graph was plotted using GraphPad Prism 5. Transcriptional level of Cyclin D1, c-Myc, COX-2, MMP-7, MMP-14 and Claudin-1 were analyzed by (d) semi-quantitative PCR and (e) real-time PCR method in control and β-Catenin knocked-down cells after challenging with FVIIa. (f) Expression profile of the downstream members was analyzed at protein level after 8 hrs of ligands addition by western blotting. (g) Protein level expression of these genes was checked in either LY294002 pre-treated or β-Catenin knock-down cells after treatment with FVIIa or PAR2AP. All the experiments were performed at least for three times. The data presented here are as mean ±S.E. of the mean. The differences are considered to be statistically significant at $p < 0.05$ using student's t-test.

Figure 7. **PAR2 activation promotes migration and invasion of MDA-MB-231 cells through PI3K-AKT dependent β-catenin accumulation.** (a) MDA-MB-231 cells were seeded on cover-glasses and grown till confluency, a single scratch line was created followed by FVIIa or PAR2AP treatment. LY294002 was added 1 hr before ligand addition. Cells were allowed to migrate to the scratched area for 36 hrs and images were taken at 0 hr and 36 hrs. Vertical black lines indicate the boundary of the edges of the wound at 0 hr, scale bar 200 μm. (b) Number of cells migrated to the scratched area were counted and graphically represented using GraphPad Prism 5. (c) Similarly, scratch migration assay was performed on control, β-catenin or PAR2 knock-down cells after challenging with FVIIa or PAR2AP, scale bar 200 μm. (d) Number of cells migrated to the scratched area were counted and graphically represented using GraphPad Prism 5. (e) Control or β-catenin knock-down cells were seeded on a transwell membrane previously coated with matrigel. Cells were treated with FVIIa or PAR2AP and incubated for 24 hrs. LY294002 was added 1 hr prior to ligand addition. The extravasated cells were stained with crystal violet and borate solution after scraping off the cells from upper chamber (as mentioned in materials and methods). Images were taken by a bright field microscope, scale bar 200 μm (f) from which the number of cells invaded were counted and graphical representation was made using GraphPad Prism 5. The experiments were performed at least thrice and data presented here as mean ±S.E. of the mean. The differences are considered to be statistically significant at $p < 0.05$ using student's t-test.

Figure 8. **Expression of β-catenin and its downstream members in human breast cancer and normal breast tissues.** Human breast cancer and normal tissue samples were collected from 5 different human breast cancer patients and were subjected to further analyses. (a) Immunohistochemistry analysis against β-Catenin, Hematoxylin and Eosin staining was done (as mentioned in materials and methods) to estimate the level of β-Catenin in human breast cancer with respect to normal breast tissue. Images were taken by a

bright field microscope under 40X resolution. (b) Expression profile of Cyclin D1, c-Myc, COX-2, MMP7, MMP14 and Claudin1 along with TF and β-Catenin was analyzed at protein level by western blotting. (c) Transcriptional level of these β-Catenin downstream members was analyzed by real time PCR. Normal tissues were obtained from same individual patient's amputed breast tissue. The experiments were performed at least thrice and data presented here as mean ±S.E. of the mean. Differences are considered to be statistically significant at $p < 0.05$ using student's t-test.

Figure 9. **Schematic representation of TF-FVIIa-dependent PAR2-activated signaling pathway which accounts for β-Catenin accumulation and expression of metastatic proteins leading to enhanced migration and invasion of human breast cancer cells.** In normal condition, GSK3β binds to Axin and APC to form "Active Phosphorylation Complex" which readily phosphorylates β-Catenin leading to its proteasomal degradation. In presence of FVIIa, active TF-FVIIa complex is being formed which activates PAR2 receptor and leads to intracellular activation of AKT via phosphorylation which again phosphorylates GSK3β and inactivates it. As a result, β-Catenin remains in a non-degradable un-phosphorylated state and accumulates inside the cell nucleus to promote the expression of several pro-metastatic genes like Cyclin D1, c-Myc, COX-2, MMP-7, MMP-14 and Claudin-1 leading to enhanced cell migration and invasion of breast cancer cells.

Figure 1.

-

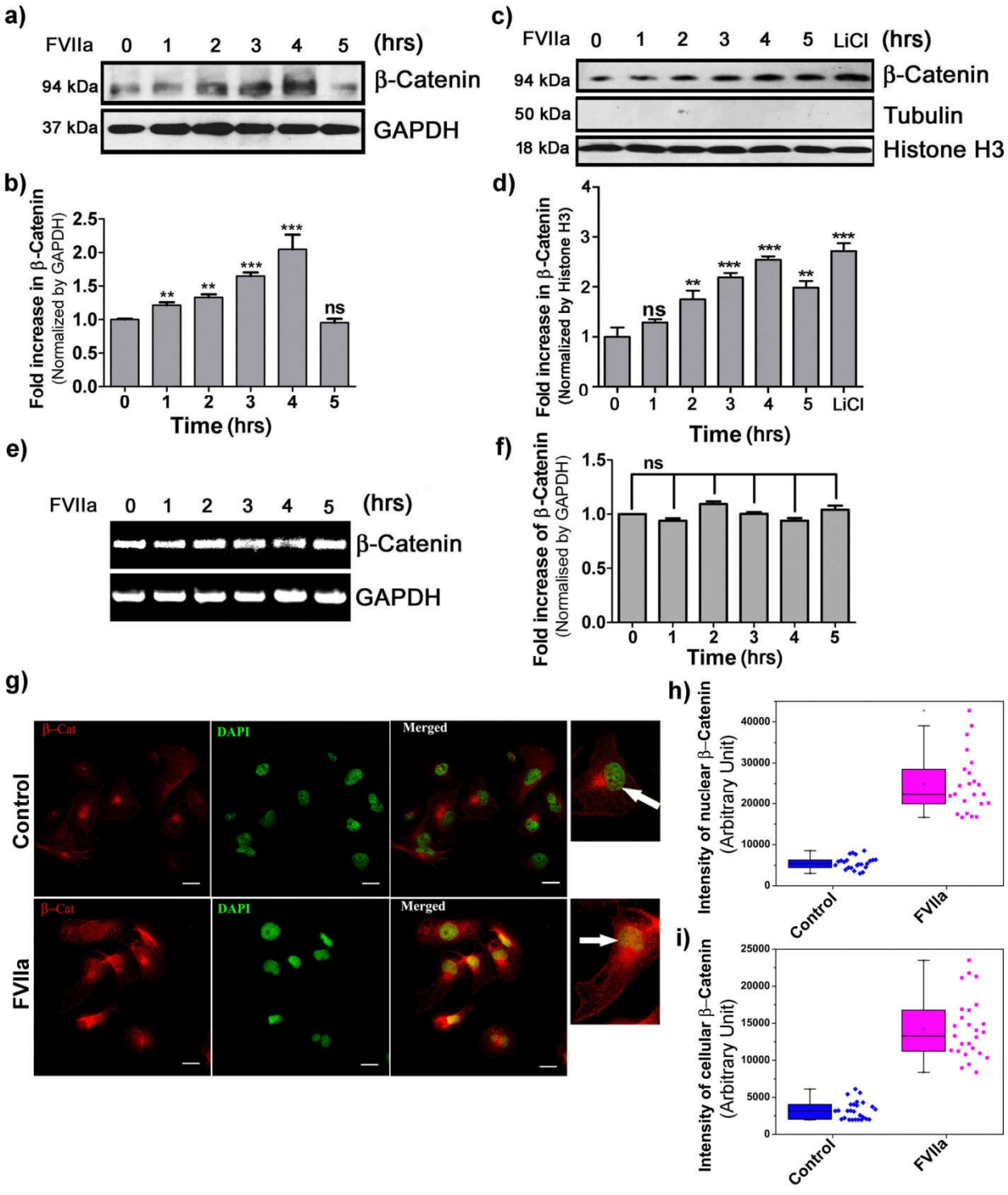

Figure 2.

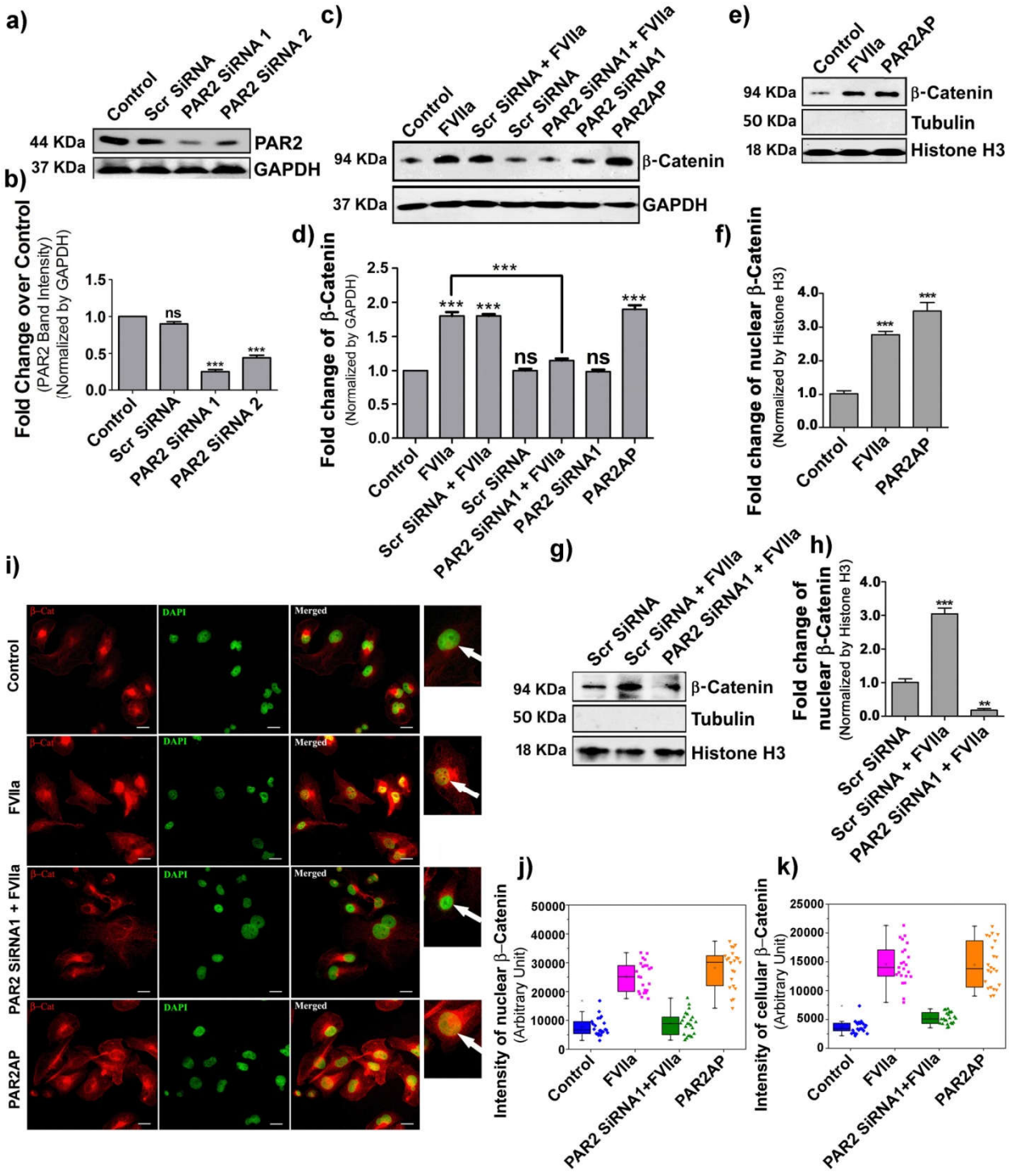

Figure 3.

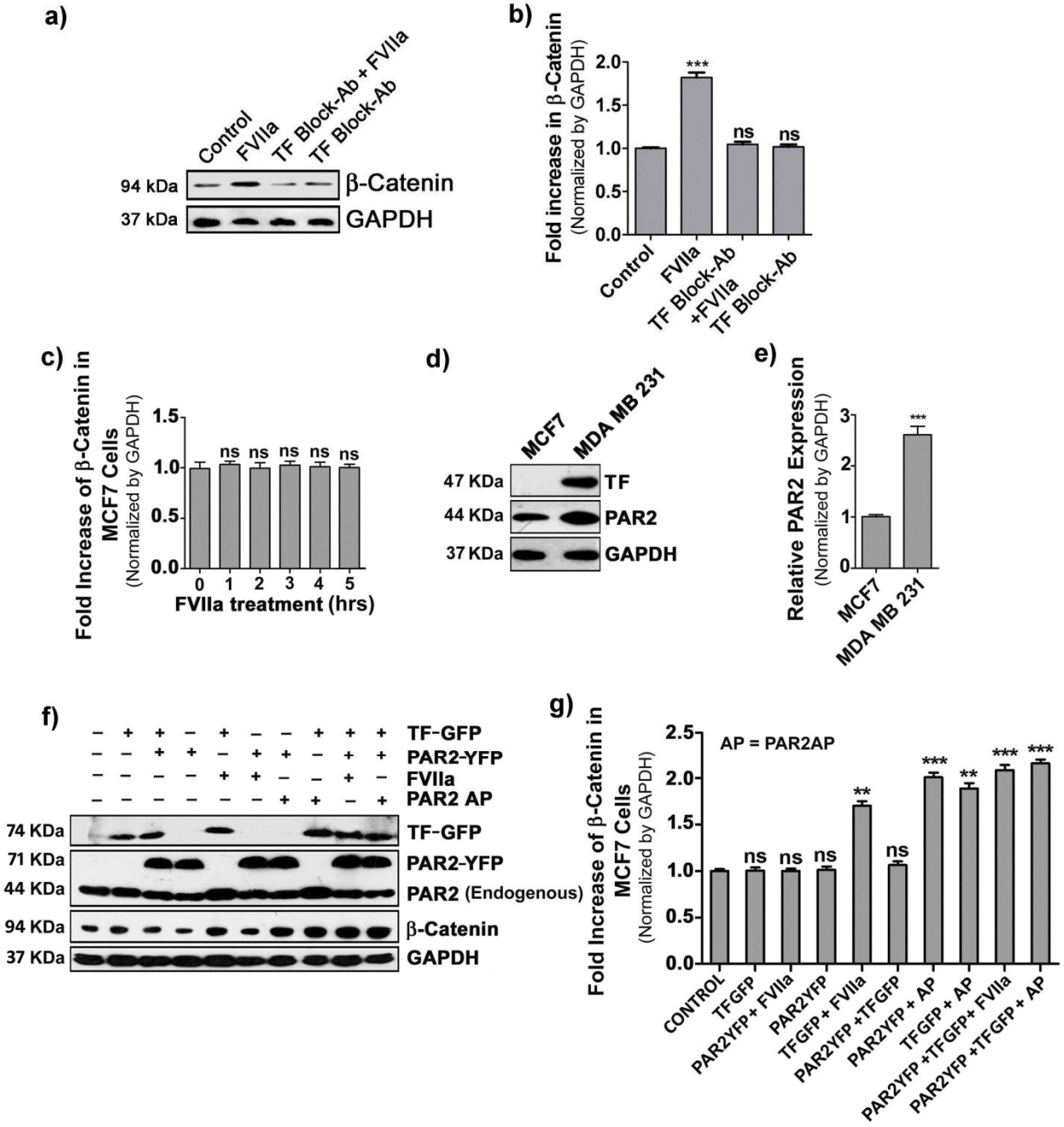

Figure 4.

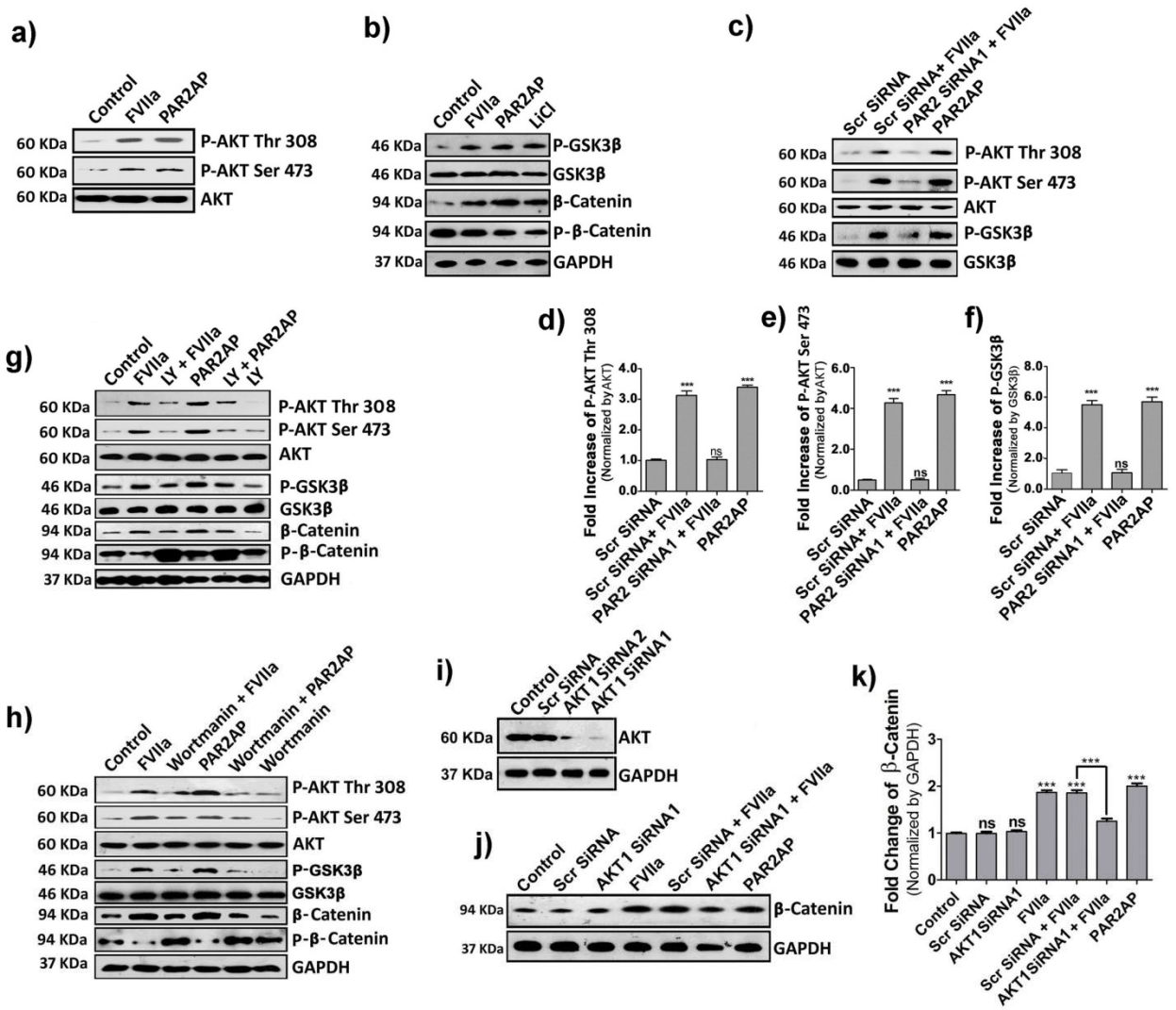

Figure 5.

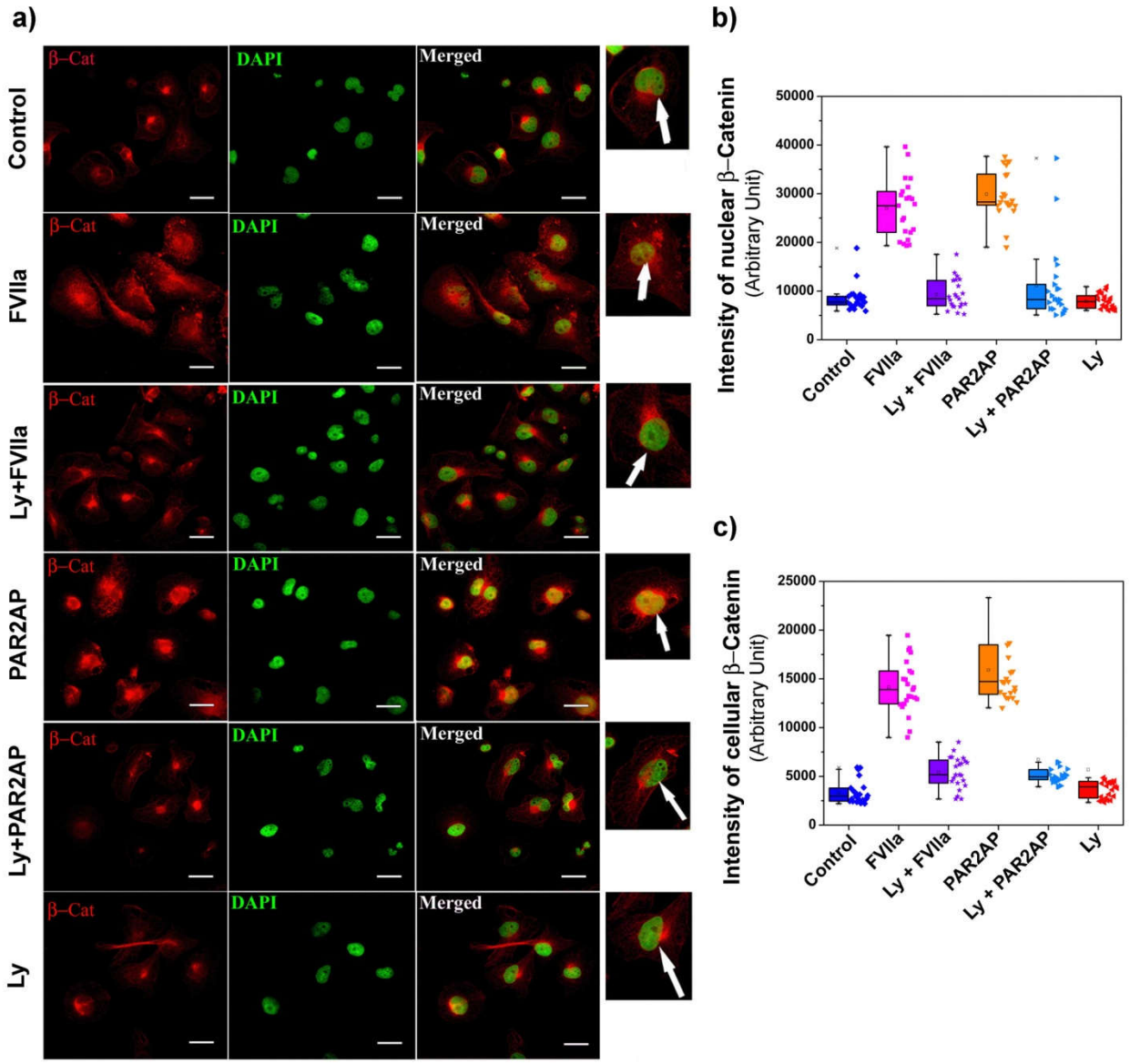

Figure 6.

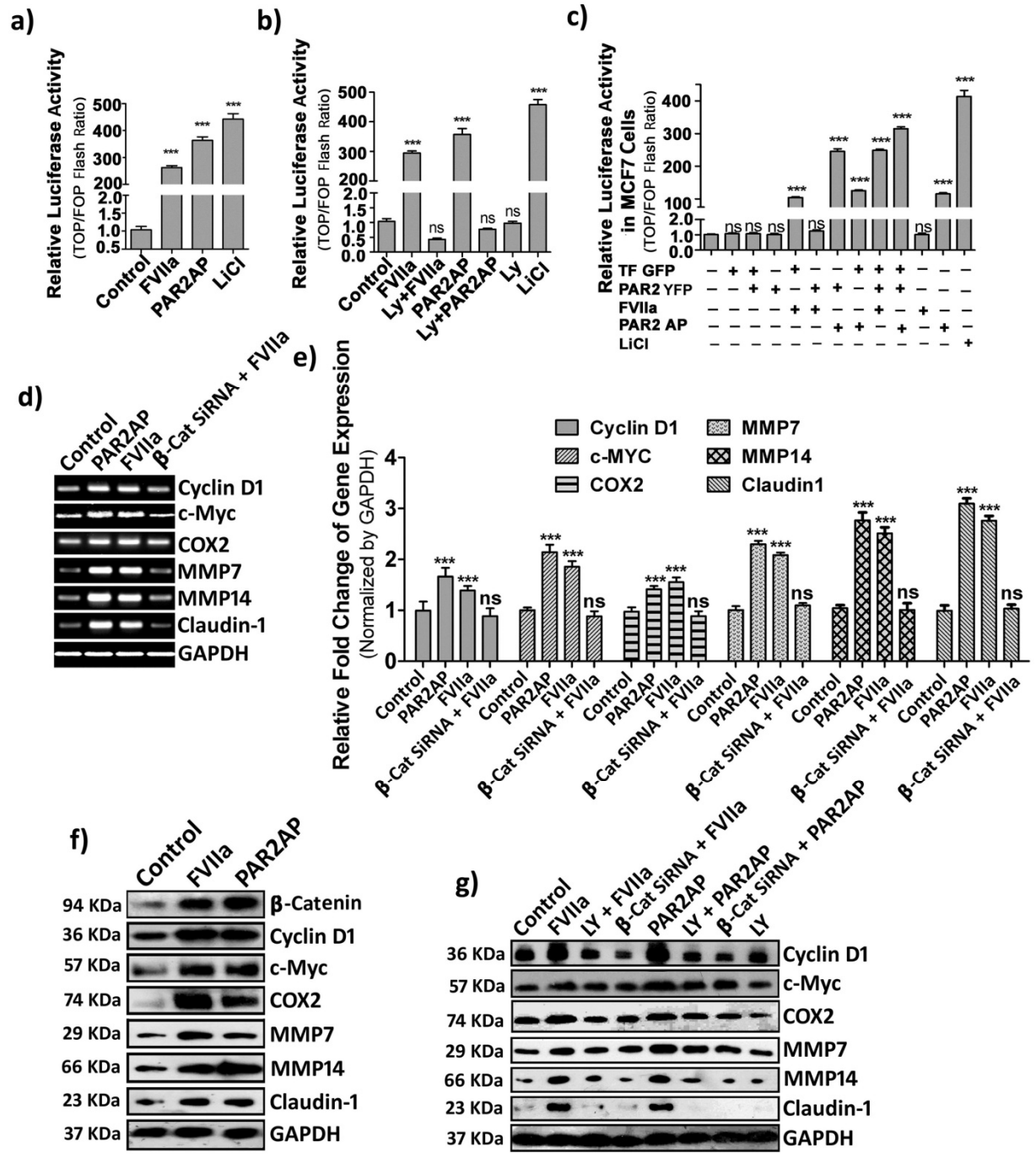

Figure 7.

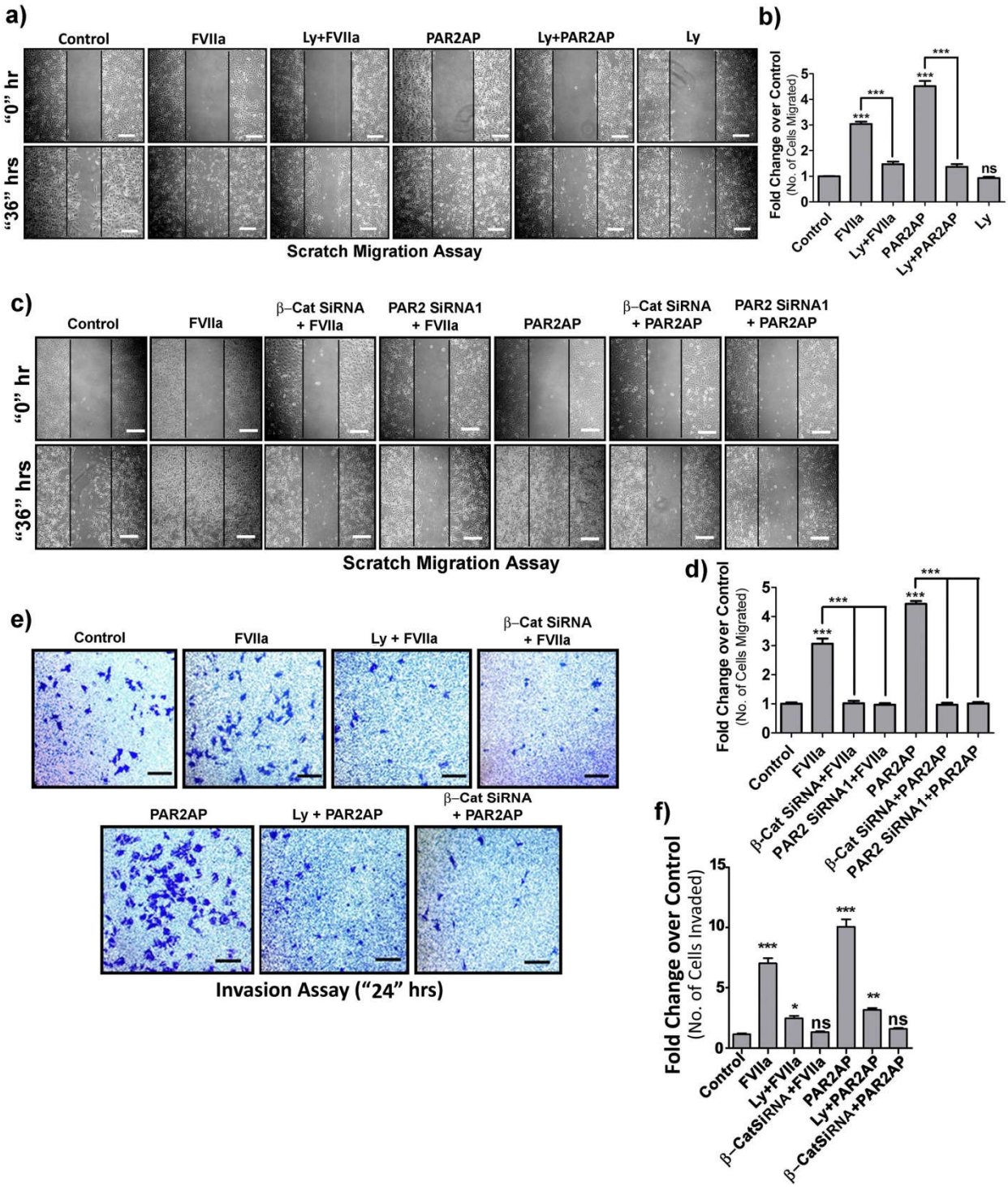

Figure 8.

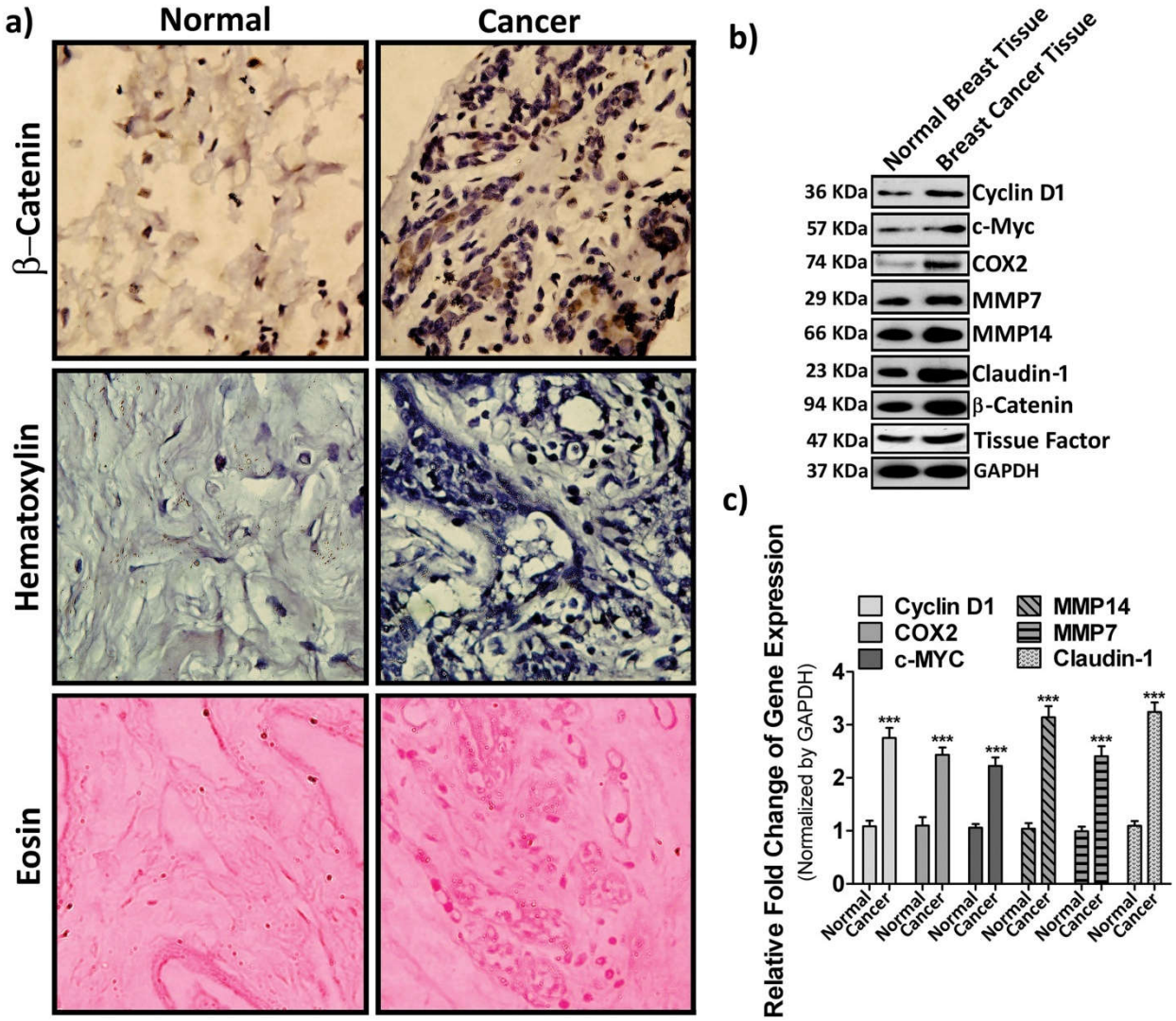

Figure 9.

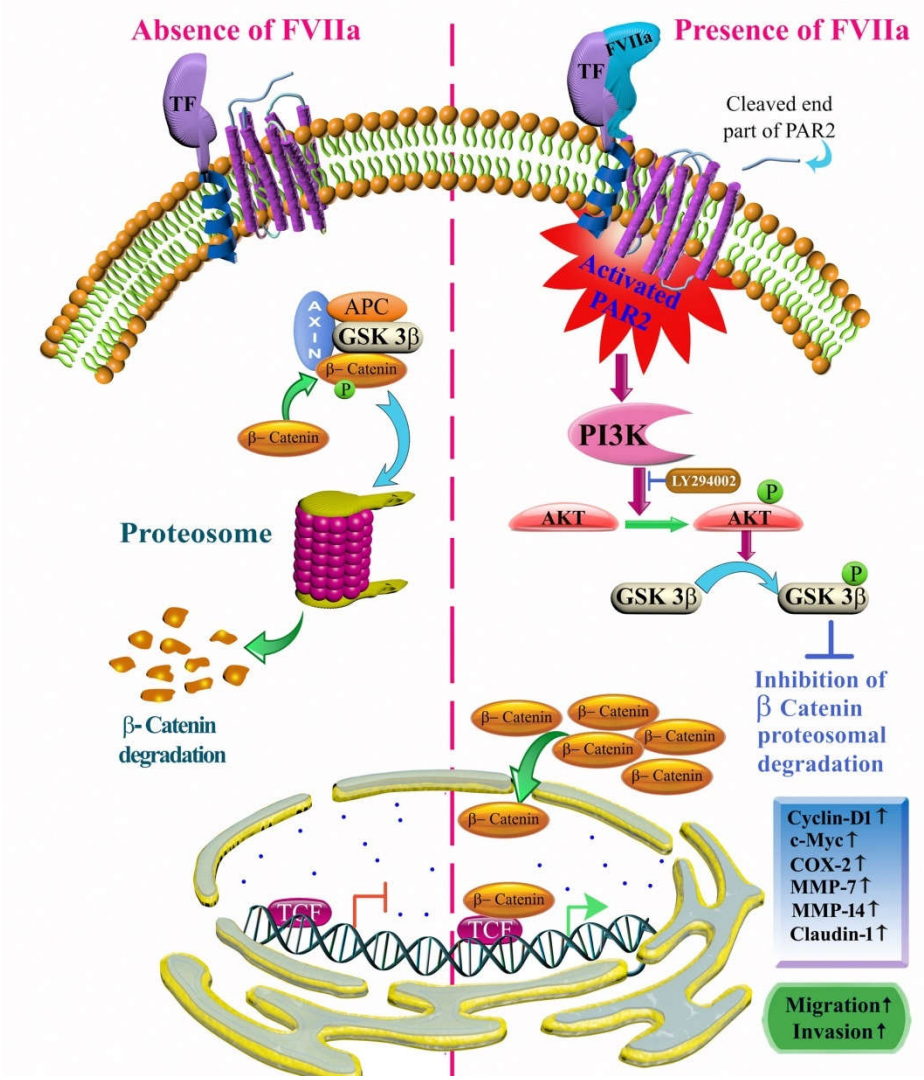

Coagulation factor VIIa-mediated protease-activated receptor 2 activation leads to β -catenin accumulation via the AKT/GSK3β pathway and contributes to breast cancer progression

Abhishek Roy, Shabbir A. Ansari, Kaushik Das, Ramesh Prasad, Anindita Bhattacharya, Suman Mallik, Asis Mukherjee and Prosenjit Sen

J. Biol. Chem. published online May 18, 2017

Access the most updated version of this article at doi: 10.1074/jbc.M116.764670